Aalborg Universitet

AALBORG UNIVERSITY

Remote Voltage Control Using the Holomorphic Embedding Load Flow Method

Liu, Chengxi; Qin, Nan; Sun, Kai; Bak, Claus Leth

Published in:
I E E E Transactions on Smart Grid

DOI (link to publication from Publisher):
10.1109/TSG.2019.2901865

Publication date:
2019

Document Version
Accepted author manuscript, peer reviewed version

Link to publication from Aalborg University

Citation for published version (APA):
Liu, C., Qin, N., Sun, K., & Bak, C. L. (2019). Remote Voltage Control Using the Holomorphic Embedding Load Flow Method. *I E E E Transactions on Smart Grid*, *10*(6), 6308 - 6319. Article 8653430. https://doi.org/10.1109/TSG.2019.2901865

General rights
Copyright and moral rights for the publications made accessible in the public portal are retained by the authors and/or other copyright owners and it is a condition of accessing publications that users recognise and abide by the legal requirements associated with these rights.

- Users may download and print one copy of any publication from the public portal for the purpose of private study or research.
- You may not further distribute the material or use it for any profit-making activity or commercial gain
- You may freely distribute the URL identifying the publication in the public portal -

Take down policy
If you believe that this document breaches copyright please contact us at vbn@aub.aau.dk providing details, and we will remove access to the work immediately and investigate your claim.

Downloaded from vbn.aau.dk on: June 18, 2025

This article has been accepted for publication in a future issue of this journal, but has not been fully edited. Content may change prior to final publication. Citation information: DOI 10.1109/TSG.2019.2901865, IEEE Transactions on Smart Grid

Remote Voltage Control Using the Holomorphic Embedding Load Flow Method

Chengxi Liu *Senior Member IEEE*, Nan Qin *Member IEEE*, Kai Sun, *Senior Member IEEE* and Claus Leth Bak, *Senior Member IEEE*

***Abstract*--This paper proposes a new remote voltage control approach based on the non-iterative holomorphic embedding load flow method (HELM). Unlike traditional power-flow based methods, this method can guarantee the convergence to the stable upper branch solution if it exists and does not depend on an initial guess of the solution. Bus type modifications are set up for remote voltage control. A participation factor matrix is integrated into the HELM to distribute reactive power injections among multiple remote reactive power resources so that the approach can remotely control the voltage magnitudes of desired buses. The proposed approach is compared with a conventional Newton-Raphson (N-R) approach by study cases on the IEEE New England 39-bus system and the IEEE 118-bus system under different conditions. The results show that the proposed approach is superior over the N-R approach in terms of tractability and convergence performance.**

***Index Terms*—Holomorphic embedding load flow method, power flow analysis, remote voltage control.**

NOMENCLATURE

P_i, Q_i, V_i	Active power injection, reactive power injection and voltage at bus i.
Y_{ik}, G_{ik}, B_{ik}, δ_{ik}	Admittance, conductance, susceptance and angle differences between buses i and k.
$\lvert V_i^{sp}\rvert$	Specified voltage magnitude at PV bus i.
V_i^{SL}	Specified voltage of the slack bus i.
Y_{ik}^{tr}	Series admittance between bus i and k
Y_i^{sh}	Shunt admittance part at bus i
s	Embedded variable.
$V[m]$	The m^{th} order power series coefficient of voltage.
N_{pvq}	Number of PVQ/P groups.
N_p	Number of P buses in each PVQ/P group.
$\mathbf{K_{p,pvq}}$	Participation factor matrix for all the N_{pvq} PVQ/P groups.
$\mathbf{K}_r$	Participation factor vector of the r^{th} PVQ/P group.
$\kappa_{r,t}$	Participation factor of the t^{th} P bus in the r^{th} PVQ/P group
$\mathcal{PQ}$, $\mathcal{PV}$, $\mathcal{SL}$	Sets of the PQ buses, PV buses and slack buses.
$\mathcal{PVQ}$, $\mathcal{P}$	Sets of the PVQ buses and P buses.

This work was supported in part by the ERC Program of the NSF and DOE under *NSF grant EEC*-1041877 and in part by *NSF grant ECCS*-1610025.

C. Liu is with the Department of Energy Technology, Aalborg University, Aalborg, Denmark and the School of Electrical Engineering and Automation, Wuhan University, Wuhan, China (email: cli@et.aau.dk).

N. Qin is with the Department of Network Planning, Energinet.dk, Fredericia, Denmark (email: naq@energinet.dk).

K. Sun is with the Department of EECS, University of Tennessee, Knoxville, TN, USA (email: kaisun@utk.edu).

C. L. Bak is with the Department of Energy Technology, Aalborg University, Aalborg, Denmark (email: clb@et.aau.dk).

I. INTRODUCTION

WITH the growing energy crisis and increasingly severe environmental pollution on the earth, more and more distributed energy resources (DERs) are integrated into electric power systems. Under this trend, not only the active power resources, but also the ancillary services, previously provided by conventional power plants, are gradually being replaced by the DERs-based power plants. The voltage control at specified buses, as one of the most important ancillary services, will be an obligation in modern power systems for the DERs-based power plants. For example, Energinet—the Danish TSO, requests that wind power plants above 11kW should be equipped with voltage control functions capable of controlling the voltage at the point of common coupling (PCC) or the reference point via activation orders [1]. In addition, DERs-based power plants are coordinated by the grid-level Automatic Voltage Control (AVC) systems that typically apply a hierarchical structure to maintain voltages at remote "pilot buses" by dispatching the set points of a variety of reactive power resources [2].

For a large-scale power grid, an advisable scheme for coordinated voltage control is to decompose the entire grid into control regions and to regulate voltages on some of buses in each region so as to reduce large reactive power exchanges between regions. For instance, reference [3] proposes an improved secondary voltage control method using feedback control to reduce reactive power exchanges through tie lines.

This paper aims at achieving accurate, fast, online remote voltage control for a regional power grid or a control region of an interconnected power grid. The voltage control is critical in the operational environment for the utilities to provide system operators with first-hand advices on control actions. The power flow calculation considering remote control is one of the most fundamental measures to maintain the voltage magnitudes of specific buses in a power grid.

A more general systematic remote voltage control strategy provided by multiple reactive power resources should be considered and integrated into the power flow calculation. For the exiting Newton-Raphson (N-R) based methods, remote voltage control requires a derivative Jacobian matrix including the sensitivity of the reactive power mismatch at the controlled buses w.r.t. the voltage at the controlling buses. Moreover, if the voltage is maintained by several controlling buses, then a distribution of the reactive power contribution is required, which significantly reduces the convergence speed as the

U.S. Government work not protected by U.S. copyright.

This article has been accepted for publication in a future issue of this journal, but has not been fully edited. Content may change prior to final publication. Citation information: DOI 10.1109/TSG.2019.2901865, IEEE Transactions on Smart Grid

quadratic convergence rate of the N-R method is downgraded to a linear convergence rate. In addition, the tractability can be weaker due to the adaption of the classical load flow method to include the remote voltage control functions. Therefore, a reliable power flow calculation integrated with remote voltage control is strongly in demand. Iterative power flow calculation methods, e.g. the N-R method, have been widely adopted by many commercialized power system software tools [4]. It is a tangent-based searching method that iteratively calculates the adjustment quantities for unknown voltage vectors based on the known power mismatch values, which requires that given initial guesses for the unknown variables are sufficiently close to the solutions. Poor initial guesses, high R/X ratios and heavy load can lead to an ill-conditioned Jacobian matrix, resulting in poor tractability [5].

The holomorphic embedding load flow method (HELM) proposed by [6]-[8] is a non-iterative method to solve the AC power flow equations (for short, PFEs). In contrast to the traditional N-R method and the existing analytical methods, the HELM provides solutions in a recursive manner, which is independent of initial guesses. It can guarantee to find a power flow solution corresponding to the stable system equilibrium if it physically exists. The HELM was firstly demonstrated on systems having only PQ buses and a slack bus [6], and then on systems having PV buses as well [7]-[15]. Researchers derive other holomorphic embedding methods for different applications including online voltage stability assessment [16], calculating the power-voltage (P-V) curves [17], probabilistic power flow [18], power flow analysis of hybrid AC/DC systems [19], finding unstable equilibrium points [20] and network reduction [21], etc.

This paper proposes remote voltage control method based on the non-iterative HELM, for controlling voltage magnitudes at specified buses in the grid using the local reactive power resources. The remote voltage control concept is firstly embedded into power flow calculations. Then, a general HELM based remote voltage control method utilizing reactive power resources from multiple remote buses is introduced, which applies a matrix of participation factors to distribute reactive power outputs among multiple reactive power resources. The matrix of participation factors is directly integrated into the HELM, succeeding its property in terms of the ability to guarantee a converged power flow solution if it exists. The case studies are carried out on the IEEE New England 39-bus system and IEEE 118-bus system under different conditions. The proposed HELM-based remote voltage control approach is compared with a traditional N-R based approach to demonstrate its superiority in terms of the tractability and convergence performance.

The major contributions of this paper include: 1) defining an embedding method for remote voltage control including bus-type modifications; 2) proposing an embedding method for the cases with participation factors, i.e. a systematic remote voltage control strategy provided by multiple reactive power resources; 3) showing its superiority over the N-R method on convergence performance.

Unlike authors' existing works [15]-[16] using a derived physical germ solution for voltage stability assessment and multi-dimensional analytical power flow solutions, this paper aims at solving PFEs with remote voltage control functions at a specific operating condition. Therefore, a generic germ solution with all voltages at $1\angle 0°$ p.u. is used, which is the fastest germ solution to obtain. Furthermore, it can also guarantee the convergence to any upper-branch solution of a P-V curve. Unlike the "initial guess" with the N-R method for iterative power flow calculations, the "germ solution" with the HELM is not required to be close enough to the desired true solution. In addition, since the HELM is based on the theory of analytical continuation, the voltages starting from the germ solution cannot go beyond the saddle-node bifurcation point on the P-V curve. The mathematical proof of convergence to a desired upper-branch solution is given in the Appendix-B.

Different from the existing methods for remote voltage control [22]-[24], which involve iterative computations, this approach does not depend on the initial guess of the solution and guarantees the convergence to the upper branch solution. In addition, the participation factors of reactive power are embedded in the whole process of the power flow calculation, aiming at accelerating the convergence.

The rest of the paper is organized as follows. Section II introduces a conventional HELM. Section III first briefly introduces remote voltage control using traditional power flow calculation and then proposes a non-iterative approach extending the HELM for coping with the remote voltage control function. Section IV verifies the proposed approach and compares it with the N-R method via the study cases on the test systems. Section V draws conclusions.

II. Conventional Holomorphic Embedding Load Flow Method

A. Principle Theory of the HELM

As shown in Fig. 1, the idea of the HELM is to embed a complex variable s into the nonlinear PFEs such that in the complex s-plane, an analytical solution is originated from a germ solution at $s = 0$ and expanded to the final solution at $s = 1$ by analytical continuation.

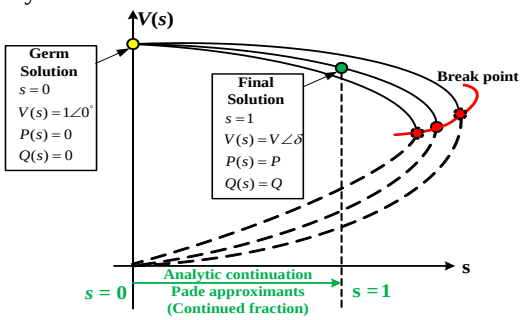

Fig. 1. The illustration of the HELM's concept.

A *holomorphic function* is a complex-valued function about one or more complex variables and is *complex-differentiable* in the neighborhood of every point in its domain. Consider a complex-valued function $x(s)$ of a complex variable $s = p+iq$, with real part p and imaginary part q. If the embedded complex-valued function $x(p+iq)$ satisfies *Cauchy-Riemann*

U.S. Government work not protected by U.S. copyright.

This article has been accepted for publication in a future issue of this journal, but has not been fully edited. Content may change prior to final publication. Citation information: DOI 10.1109/TSG.2019.2901865, IEEE Transactions on Smart Grid

Equation (1), then $x(s)$ is *complex-differentiable* and thus *holomorphic* in a neighborhood of the s-plane [25].

$$i\frac{\partial x}{\partial p}=\frac{\partial x}{\partial q} \tag{1}$$

Under this circumstance, $x(s)$ can be represented in the form of power series (2) in s within its convergence region $\boldsymbol{C}$ [26].

$$x(s)=\sum_{m=0}^{\infty}x[m]s^m, s\subset\boldsymbol{C} \tag{2}$$

In order to solve a nonlinear equation $g(x) = 0$, substitute (2) for x to generate a composite function of embedded variable s:

$$g\left(x\right)=g\left[x(s)\right]=0 \tag{3}$$

Therefore, the power-flow problem becomes how to design an $x(s)$ satisfying the following four criteria:

1) A *germ* solution having $s = 0$ can be found for (3). For power flow calculation, the germ solution is conventionally designated as the solution under a no-load, no-generation condition.
2) Eq. (3) also holds at $s = 1$ and the power series (2) can be induced within a defined number of order, through expanding and equating the coefficients of the same order of s^m in (3). Thus, the final solution of x is obtained with $s = 1$ in (2).
3) The s-embedded complex function $g[x(s)]$ is analytically continuous (*holomorphic*) along the path from the germ solution at $s = 0$ to the final solution at $s = 1$.
4) On the path of s before bifurcation occurs, there is no exceptional point (also called the branch point) where multiple solutions of $g[x(s)] = 0$ coalesce with each other. Exceptional points only coincide at the bifurcation point.

B. HELM's Canonical Embedding

Consider an N-bus system composed of PQ buses, PV buses and slack bus, which are denoted as sets of $\boldsymbol{\mathcal{PQ}}$, $\boldsymbol{\mathcal{PV}}$ and $\boldsymbol{\mathcal{SL}}$, respectively. The original PFEs for PQ buses, PV buses and slack bus are expressed respectively by

$$\sum_{k=1}^{N}Y_{ik}V_k=\frac{S_i^*}{V_i^*},\forall i\in\boldsymbol{\mathcal{PQ}} \tag{4}$$

$$\begin{cases}P_i=\mathrm{Re}\left(V_i\sum_{k=1}^{N}Y_{ik}^*V_k^*\right)\\ \left|V\right|_i=\left|V_i^{sp}\right|\end{cases},\forall i\in\boldsymbol{\mathcal{PV}} \tag{5}$$

$$V_i=V_i^{SL},\forall i\in\boldsymbol{\mathcal{SL}} \tag{6}$$

where P_i, Q_i and V_i are the active and reactive power injections and voltage at bus i, Y_{ik} is the admittance between buses i and k, $|V_i^{sp}|$ is the specified voltage magnitude at PV buses and V_i^{SL} is the given slack bus voltage. "Re" takes the real part.

The HELM's *canonical embedding* is proposed in [8], where the admittance Y_{ik} is split to the transmission admittance part, i.e. Y_{ik}^{tr}, comprising of the series admittance between buses i and k, and the shunt admittance part, i.e. Y_i^{sh}, composed of the branches charging and shunt admittances at buses i, respectively. Moreover, the voltage of each bus and the reactive power of each PV bus are both represented as power series functions of an embedded complex variable s, denoted by $V(s)$ and $Q(s)$ respectively. Then, the s-embedded equations of PQ buses, PV buses and SL buses in (4)-(6) can be expressed as (7)-(9) respectively. Note that, to maintain the holomorphy of $V(s)$, its conjugate function is $V^*(s^*)$.

$$\sum_{k=1}^{N}Y_{ik}^{tr}V_k(s)=\frac{sS_i^*}{V_i^*(s^*)}-sY_i^{sh}V_i(s),\forall i\in\boldsymbol{\mathcal{PQ}} \tag{7}$$

$$\begin{cases}\sum_{k=1}^{N}Y_{ik}^{tr}V_k(s)=\frac{sP_i-jQ_i(s)}{V_i^*(s^*)}-sY_i^{sh}V_i(s)\\ V_i(s)V_i^*(s^*)=1+\left(\left|V_i^{sp}\right|^2-1\right)s\end{cases},\forall i\in\boldsymbol{\mathcal{PV}} \tag{8}$$

$$V_i(s)=1+(V_i^{SL}-1)s,\forall i\in\boldsymbol{\mathcal{SL}} \tag{9}$$

See the conventional *canonical embedding* in TABLE I, the voltage at no load condition is assumed to be $1\angle0^\circ$ p.u.. Under this condition at $s = 0$, the voltage at the slack bus propagates to all buses, which results in all voltages are equal to $1\angle0^\circ$ p.u.. Besides, the original problem is recovered at $s = 1$, which leads to the voltage changes at all buses.

TABLE I. THE EMBEDDING OF POWER FLOW EQUATIONS FOR PQ, PV AND SLACK BUSES WITH THE CONVENTIONAL HELM [9]

Type	Germ Solution ($s = 0$)	Holomorphic Embedding Method ($s = 1$ for the original PFEs)
SL	$V_i(s)=1$	$V_i(s)=1+(V_i^{SL}-1)s$
PQ	$\sum_{k=1}^{N}Y_{ik}^{tr}V_k(s)=0$	$\sum_{k=1}^{N}Y_{ik}^{tr}V_k(s)=\frac{sS_i^*}{V_i^*(s^*)}-sY_i^{sh}V_i(s)$
PV	$\sum_{k=1}^{N}Y_{ik}^{tr}V_k(s)=0$ $V_i(s)\cdot V_i^*(s)=1$	$\sum_{k=1}^{N}Y_{ik}^{tr}V_k(s)=\frac{sP_i-jQ_i(s)}{V_i^*(s^*)}-sY_i^{sh}V_i(s)$ $V_i(s)\cdot V_i^*(s^*)=1+\left(\left\|V_i^{sp}\right\|^2-1\right)s$

The unknown voltages and reactive power injections at PV buses can be expanded to the power series w.r.t. s, i.e. the Taylor series for the voltage and reactive power at PV buses in (10) and (11). The complex conjugate of voltage reciprocal on the right hand side of (7)-(9) $1/V^*(s^*)$ are defined as (12), which converts polynomial division to convolution operation, and then finds the recursive pattern of complex voltage functions w.r.t s.

$$V_i(s)=\sum_{m=0}^{\infty}V_i[m]s^m \tag{10}$$

$$Q_i(s)=\sum_{m=0}^{\infty}Q_i[m]s^m \tag{11}$$

$$W_i^*(s)=1/V_i^*(s^*)=\sum_{m=0}^{\infty}W_i^*[m]s^m \tag{12}$$

After plugging (10)-(12) into (7)-(9), power series coefficients are obtained by differentiating equations w.r.t s on both sides and equating coefficients of s, s^2,… up to s^m. This procedure recursively calculates $V[m]$ and $Q[m]$ using the previous coefficients $V[0]$, …, $V[m\text{-}1]$ and $Q[0]$, …, $Q[m\text{-}1]$. More details can be found in [9].

III. INTEGRATION OF REMOTE VOLTAGE CONTROL INTO POWER FLOW CALCULATION

A. Remote Voltage Control Based on Traditional N-R Method

The N-R method for solving AC PFEs is an iterative method that linearizes the nonlinear PFEs (13) at each

U.S. Government work not protected by U.S. copyright.

This article has been accepted for publication in a future issue of this journal, but has not been fully edited. Content may change prior to final publication. Citation information: DOI 10.1109/TSG.2019.2901865, IEEE Transactions on Smart Grid

iteration. Normally, the active power and the reactive power generations and consumptions at PQ buses, the active power generations and the voltage magnitudes at PV buses are given. The iteration starts from initial guesses for unknown network variables and stops if the active power mismatches at PQ and PV buses and the reactive power mismatches at PQ buses are smaller than the error tolerance.

$$P_i = |V_i| \sum_{k=1}^{N} |V_k| \left(G_{ik} \cos \delta_{ik} + B_{ik} \sin \delta_{ik} \right) \qquad (13)$$

$$Q_i = |V_i| \sum_{k=1}^{N} |V_k| \left(G_{ik} \sin \delta_{ik} - B_{ik} \cos \delta_{ik} \right)$$

In (13), P_i and Q_i are the net active and reactive power injections at bus i. V_i and V_k are the complex bus voltages. G_{ik}, B_{ik} and δ_{ik} are the conductance, susceptance and voltage angle difference between buses i and k, respectively.

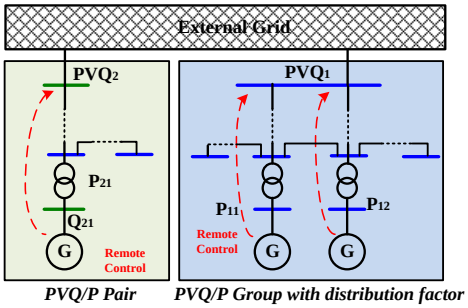

Fig. 2. The illustration of generators' remote voltage control functions.

The traditional "PV bus" is used for local voltage control. Nevertheless, in some practical applications, the voltage magnitudes at some buses are remotely controlled by one generator or a group of generators [22]. As shown in Fig. 2, the bus under control is typically an important load bus, e.g. a pilot bus in the AVC system. In the case of a load bus under remote voltage control, this bus becomes a PVQ bus, as its active power P_i, reactive power Q_i and voltage magnitude $|V_i|$ are all given. The generator bus controlling that load bus will change from a PV bus to a P bus, as the generators' reactive power is under control to meet the voltages of the PVQ bus. The voltage magnitude at the P bus is therefore unknown. The remote voltage control by a single generator is illustrated as the "*PVQ/P pair*" on the left-hand side of Fig. 2.

In the case that several generators jointly control the voltage at a remote PVQ bus, participation factors of all generators are specified for allocating their reactive power outputs. Therefore, the PVQ bus and those generator buses (i.e. P buses) are grouped, i.e. "*PVQ/P group*" shown on the right-hand side of Fig. 2, where the voltage magnitudes at PVQ buses are maintained by the corresponding generators at P buses. The set-up of "*PVQ/P groups*" is important [23]-[24]. For some power systems, the power plants are not fully controlled by the system operators. Only the voltage of PCC is assessable from the control center. Without the set-up of "*PVQ/P groups*", the only way to implement remote voltage control is to adjust reactive powers of generators for the voltage at PCC to approach the reference. It is not able to exactly and timely warrant the PCC voltage magnitude to be the reference value.

The traditional approach based on the N-R method is extended to include the PVQ and P buses. The main extension is to apply the sensitivity of the reactive power output at a PVQ bus w.r.t. the relevant P bus voltage magnitude in the iteration process. The complete formulation including the new type of buses in the iteration process can be presented by (14).

$$\begin{bmatrix} \Delta \mathbf{P_m} \\ \Delta \mathbf{Q_n} \end{bmatrix} = \begin{bmatrix} \frac{\partial \mathbf{P_m}}{\partial \boldsymbol{\delta}_{\mathbf{pv}}} & \frac{\partial \mathbf{P_m}}{\partial \boldsymbol{\delta}_{\mathbf{pq}}} & \frac{\partial \mathbf{P_m}}{\partial \boldsymbol{\delta}_{\mathbf{p}}} & \frac{\partial \mathbf{P_m}}{\partial \boldsymbol{\delta}_{\mathbf{pvq}}} & \frac{\partial \mathbf{P_m}}{\partial \mathbf{V}_{\mathbf{pq}}} & \frac{\partial \mathbf{P_m}}{\partial \mathbf{V}_{\mathbf{p}}} \\ \frac{\partial \mathbf{Q_n}}{\partial \boldsymbol{\delta}_{\mathbf{pv}}} & \frac{\partial \mathbf{Q_n}}{\partial \boldsymbol{\delta}_{\mathbf{pq}}} & \frac{\partial \mathbf{Q_n}}{\partial \boldsymbol{\delta}_{\mathbf{p}}} & \frac{\partial \mathbf{Q_n}}{\partial \boldsymbol{\delta}_{\mathbf{pvq}}} & \frac{\partial \mathbf{Q_n}}{\partial \mathbf{V}_{\mathbf{pq}}} & \frac{\partial \mathbf{Q_n}}{\partial \mathbf{V}_{\mathbf{p}}} \end{bmatrix} \begin{bmatrix} \Delta \boldsymbol{\delta}_{\mathbf{pv}} \\ \Delta \boldsymbol{\delta}_{\mathbf{pq}} \\ \Delta \boldsymbol{\delta}_{\mathbf{p}} \\ \Delta \boldsymbol{\delta}_{\mathbf{pvq}} \\ \Delta \mathbf{V}_{\mathbf{pq}} \\ \Delta \mathbf{V}_{\mathbf{p}} \end{bmatrix} \qquad (14)$$

$$\mathbf{m} \in \{\mathbf{pv}, \quad \mathbf{pq}, \quad \mathbf{p}, \quad \mathbf{pvq}\}$$

$$\mathbf{n} \in \{\mathbf{pq}, \quad pvq_r, \quad p_{r,2}, \cdots, p_{r,t}, \cdots, p_{r,Np}\} \text{ and } r = 1 \cdots N_{pvq}$$

where **m** and **n** represent the index set of the active power and the reactive power gradients and N_{pvq} is the number of PVQ/P groups and N_p is the number of P buses in each PVQ/P group. The active power mismatches at all buses expect for the slack bus are included in **m**, whereas the reactive power mismatches only at PQ buses, PVQ buses and P buses are included in **n**.

A participation factor vector $\mathbf{K}_r$ is specified for the sharing percentages of reactive power outputs among generators in the r^{th} PVQ/P group. Hence, after each iteration, the reactive power generation among generators needs for re-dispatch according to the participation factor matrix. For the n^{th} iteration, the reactive power generation is calculated based on the results of the $(n\text{-}1)^{\text{th}}$ iteration, as defined in (15).

$$Q_{r,t}[n] = \mathbf{K}_r \sum_{t=1}^{N_p} \left(Q_{r,t}[n-1] + \Delta Q_{r,t}[n] \right) \text{ and } r = 1 \cdots N_{pvq} \qquad (15)$$

$$\mathbf{K}_r = \left[\kappa_{r,1} \quad \kappa_{r,1} \quad \cdots \quad \kappa_{r,t} \quad \cdots \quad \kappa_{r,N_p} \right]^T \qquad (16)$$

The essence of Eq. (15) is to add the reactive power variation of the n^{th} iteration, i.e. $\Delta Q_{r,t}[n]$ onto the result of the $(n\text{-}1)^{\text{th}}$ iteration, i.e. $Q_{r,t}[n\text{-}1]$, and then distribute the summation to every P bus by a participation factor vector $\mathbf{K}_r$. Eq. (16) is the vector composed of reactive power contribution in the PVQ/P group. In (15) and (16), r is the group index in the list of all PVQ/P groups, and t is the index of P buses at a certain PVQ/P group. $\mathbf{K}_r$ is the participation factor for the r^{th} PVQ/P group (16), where

$$\sum_{t=1}^{N_p} \kappa_{r,t} = 1 \qquad (17)$$

meaning that the sum of reactive power share for every P bus in the PVQ/P group is 1. The reactive power at the other P buses of the r^{th} PVQ/P group for the n^{th} iteration, i.e. $Q_{r,2}[n]$ to $Q_{r,t}[n]$, are found after the updating process via the participation factor $\mathbf{K}_r$.

The participation factor vector $\mathbf{K}_r$ is also able to distribute the reactive power supplies among generators located in one power plant or nearby multiple plants. The advantage for the division of reactive power supply among generators located at one power plant or nearby plants is to optimally allocate the reactive power reserve from each generator, which determines the ability of maintaining voltage after disturbances.

U.S. Government work not protected by U.S. copyright.

This article has been accepted for publication in a future issue of this journal, but has not been fully edited. Content may change prior to final publication. Citation information: DOI 10.1109/TSG.2019.2901865, IEEE Transactions on Smart Grid

Moreover, the reactive control scheme would impact the loss of generators, which should also be appropriately distributed among generators.

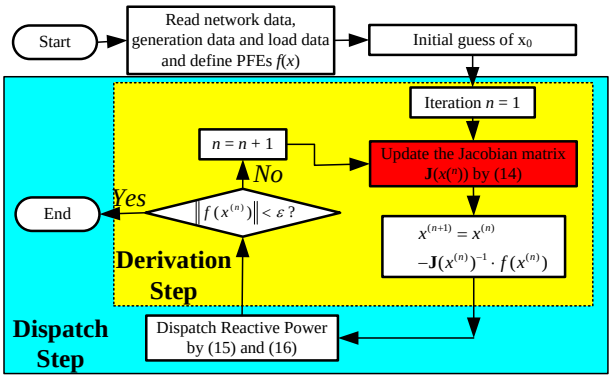

Fig. 3. Block diagram of joint remote voltage control based on N-R method.

In summary, the joint remote voltage control algorithm based on the N-R method comprises of a *derivation step* and a *dispatch step*, as shown in Fig. 3. The *derivation step* calculates the sensitivity and obtains the power mismatch, and the *dispatch step* re-dispatches the reactive power generation among generators. Because the iterations based on Eq. (15) do not utilize any gradient information towards the final solution, the overall convergence rate degrades from a quadratic rate with the N-R method to a linear rate. This can also be observed by solving the IEEE 39-bus system power flows under a normal operating condition: 4 interactions are needed by the N-R method without PVQ/P pairs while 18 iterations are needed with PVQ/P pairs.

It is possible to merge the dispatching step into the Jacobian matrix, but that is still essentially linear reallocation of the reactive power among P buses according to the reactive power mismatch of PVQ node is the same. As a result, the overall performance is basically unchanged.

B. Remote Voltage Control Based on the HELM

In the HELM, all the constraints can be integrated into the matrix equations regarding the unknown values, there is no need of additional *dispatch step* for constraints. As mentioned above, the PQ buses under remote voltage control are converted to PVQ buses. Meanwhile, the buses connected with reactive power resources are changed to P buses, accordingly. The PVQ buses and P buses are in groups. The supplementary equations to include the so called *PVQ/P groups* in HELM are presented in (18)-(19), where $\mathcal{PVQ}$ and $\mathcal{P}$ represent sets of PVQ buses and P buses respectively.

$$\begin{cases} \sum_{k=1}^{N} Y_{ik}^{tr} V_k(s) = s\dfrac{P_i - jQ_i}{V_i^*(s^*)} - sY_i^{sh} V_i(s) \\ V_i(s)V_i^*(s^*) = 1 + \left(\left|V_i^{sp}\right|^2 - 1\right)s \end{cases}, \forall i \in \mathcal{PVQ} \tag{18}$$

$$\sum_k Y_{ik}^{tr} V_k(s) = s\frac{P_i - j\kappa_i \sum_t Q_i(s)}{V_i^*(s^*)} - sY_i^{sh} V_i(s), \forall i \in \mathcal{P} \tag{19}$$

The active power and the reactive power at PVQ buses are known values. Compared with the PQ bus in Eq. (7), there is one more constraint at PVQ bus, i.e. the specified voltage magnitude in (18). This constraint is maintained by the reactive powers at P buses. The total required reactive power, i.e. $\sum Q_i(s)$ to maintain the voltage at the PVQ buses are distributed among the associated P buses with the predefined contribution factor κ_i for each PVQ/P group, as defined in (19). By equating the coefficients of power series w.r.t s on both sides and assuming $V_i[0] = 1\angle 0^\circ$ for the no load condition. The reactive power at P buses defined as new variables will be varied in order to control the voltage magnitudes at corresponded PVQ buses, with a contribution factor in order to obtain a unique solution.

C. Calculation Procedure

The complete formulations of the embedded power flow equations are presented in (7)-(9) and (18)-(19). The power series can be applied to expand the unknown variables to the power series with respect to s, and then to equate both sides of the complex-valued equations with the same order to solve the coefficients of power series terms. Similar to the mathematical induction method, the calculation of the power series coefficients is carried out order by order, i.e. from the low orders to high orders. The calculation procedure of remote voltage control in the HELM consists of the following four steps.

***Step 1*:** For the order of power series $m = 0$, similar to the "flat-start" in N-R method, assume the germ voltage at slack bus is $V_i^{SL}[0] = 1\angle 0^\circ$ for no load condition. Then the voltages at all buses are equal to V_i^{SL}. As shown in (20) and (21), for the germ solution, all the bus voltages in the network equal to 1, and the reactive powers at P buses and PV buses are 0.

$$V_i[0] = 1, \forall i \in \mathcal{N} \tag{20}$$

$$Q_i[0] = 0, \forall i \in \mathcal{P} \cup \mathcal{PV} \tag{21}$$

where $\mathcal{N}$ is the set of all buses in the system.

***Step 2*:** For the order m=1, differentiate the power flow equation w.r.t s at both sides, evaluate at $s = 0$, and substitute calculated coefficients from Step 1. Here are (22)-(27).

Slack bus: $$V_i[1] = V_i^{SL} - 1, \forall i \in \mathcal{SL} \tag{22}$$

PV buses: $$\begin{cases} \sum_{k=1}^{N} Y_{ik}^{tr} V_k[1] = P_i - Y_i^{sh} \\ V_{i,re}[1] = \dfrac{\left|V_i^{sp}\right|^2 - 1}{2} \end{cases}, \forall i \in \mathcal{PV} \tag{23}$$

PQ buses: $$\sum_{k=1}^{N} Y_{ik}^{tr} V_i[1] = (P_i - jQ_i) - Y_i^{sh}, \forall i \in \mathcal{PQ} \tag{24}$$

PVQ buses: $$\begin{cases} \sum_{k=1}^{N} Y_{ik}^{tr} V_k[1] = P_i - jQ_i - Y_i^{sh} \\ V_{i,re}[1] = \dfrac{\left|V_i^{sp}\right|^2 - 1}{2} \end{cases}, \forall i \in \mathcal{PVQ} \tag{25}$$

P buses: $$\sum_{k=1}^{N} Y_{ik}^{tr} V_i[1] = P_i - Y_i^{sh}, \forall i \in \mathcal{P} \tag{26}$$

All buses: $$W_i[1] = -W_i[0] = -1, \forall i \in \mathcal{N} \tag{27}$$

***Step 3*:** For the order of power series $m > 1$, continuously calculate finite numbers of orders using (28)-(33) until the active power mismatches at all buses except the slack bus, and the reactive power mismatches at PQ and PVQ buses are

U.S. Government work not protected by U.S. copyright.

This article has been accepted for publication in a future issue of this journal, but has not been fully edited. Content may change prior to final publication. Citation information: DOI 10.1109/TSG.2019.2901865, IEEE Transactions on Smart Grid

respectively smaller than a pre-defined error tolerance.

Slack bus:
$$V_i[m]=0,\forall i\in \boldsymbol{\mathcal{SL}} \tag{28}$$

PV buses:
$$\begin{cases}\sum_{k=1}^{N}Y_{ik}^{tr}V_k[m]=P_iW_i^*[m-1]-j\left(\sum_{\tau=1}^{m-1}Q_i[\tau]W_i^*[m-\tau]\right)\\ \qquad -Y_i^{sh}V_i[m-1]-j\mathbf{Q_i}[m] \qquad ,\forall i\in\boldsymbol{\mathcal{PV}}\\ V_{i,re}[m]=-\frac{1}{2}\left(\sum_{\tau=1}^{m-1}V_i[\tau]V_i^*[m-\tau]\right)\end{cases} \tag{29}$$

PQ buses:
$$\sum_{k=1}^{N}Y_{ik}^{tr}V_i[m]=(P_i-jQ_i)W_i^*[m-1]-Y_i^{sh}V_i[m-1],\forall i\in\boldsymbol{\mathcal{PQ}} \tag{30}$$

PVQ buses:
$$\begin{cases}\sum_{k=1}^{N}Y_{ik}^{tr}V_i[m]=(P_i-jQ_i)W_i^*[m-1]-Y_i^{sh}V_i[m-1]\\ V_{i,re}[m]=-\frac{1}{2}\left(\sum_{\tau=1}^{m-1}V_i[\tau]V_i^*[m-\tau]\right)\end{cases},\forall i\in\boldsymbol{\mathcal{PVQ}} \tag{31}$$

P buses:
$$\sum_{k=1}^{N}Y_{ik}^{tr}V_k[m]=P_iW_i^*[m-1]-j\left(\sum_{\tau=1}^{m-1}Q_i[\tau]W_i^*[m-\tau]\right) \tag{32}$$
$$-Y_i^{sh}V_i[m-1]-j\mathbf{Q_i}[m],\qquad \forall i\in\boldsymbol{\mathcal{P}}$$

All buses except for the slack bus:
$$W_i[m]=-\sum_{\tau=0}^{m-1}\frac{W_i[\tau]\cdot V_i[m-\tau]}{V_i[0]},\forall i\in\overline{\boldsymbol{\mathcal{SL}}} \tag{33}$$

The real part of the voltage variables at PV and PVQ buses in (23) and (25) for m = 1, and (29) and (31) for m > 1.

Since the reactive power $Q(s)$ at PV buses and P buses are real valued, the matrix equations (29)-(32) are separated into real and imaginary parts, respectively. The admittance matrix is also separated into real and imaginary parts as follows

$$\sum Y^{tr}V=\sum\left(\left(G^{tr}V_{re}-B^{tr}V_{im}\right)+j\left(B^{tr}V_{re}-G^{tr}V_{im}\right)\right) \tag{34}$$

Finally, Eq. (29)-(32) can be represented in (39), where the unknown reactive power injections at PV and PVQ buses are moved to the left hand side of the matrix equation, whereas the known voltage real parts at PV and PVQ buses are moved to the right hand side.

$$\boldsymbol{\mathcal{PQ}}[m-1]=(P_i-jQ_i)W_i^*[m-1]-Y_i^{sh}V_i[m-1] \tag{35}$$

$$\boldsymbol{\mathcal{PV}}[m-1]=P_iW_i^*[m-1]-j\left(\sum_{\tau=1}^{m-1}Q_i[\tau]W_i^*[m-\tau]\right)-Y_i^{sh}V_i[m-1] \tag{36}$$

$$\boldsymbol{\mathcal{PVQ}}[m-1]=(P_i-jQ_i)W_i^*[m-1]-Y_i^{sh}V_i[m-1] \tag{37}$$

$$\boldsymbol{\mathcal{P}}[m-1]=P_iW_i^*[m-1]-j\left(\sum_{\tau=1}^{m-1}Q_i[\tau]W_i^*[m-\tau]\right)-Y_i^{sh}V_i[m-1] \tag{38}$$

In (39), $\boldsymbol{\mathcal{PQ}}[m\text{-}1]$, $\boldsymbol{\mathcal{PV}}[m\text{-}1]$, $\boldsymbol{\mathcal{PVQ}}[m\text{-}1]$ and $\boldsymbol{\mathcal{P}}[m\text{-}1]$ represent the following (35), (36), (37) and (38) respectively. The unknowns $\mathbf{Q_{pv}}[m]$ and $\mathbf{Q_p}[m]$ are moved to the left hand side. $\mathbf{I_{pv,pv}}$ is an identity matrix. $Q_p[m]$ represents the total required reactive power at corresponding P buses to maintain voltages at associated PVQ buses. $\mathbf{K_{p,pvq}}$ is the participation factor matrix for all N_{pvq} PVQ/P groups, which is presented in the form of (40). To calculate m^{th} coefficients, the individual reactive power injection at each P bus, i.e. $Q_{p1}[m]$, $Q_{p2}[m]$,…, $Q_{pN}[m]$, is directly obtained via sub-matrix $\mathbf{Q_p}[m]$ in (15).

Step 4: Extend the convergence region to obtain the values.

As long as coefficients of a new order of the power series are obtained, the variables can be found by summation of their power series. However, this approach might be limited by the radius of convergence of the series [6]. Therefore, Padé approximants [27], [28] or continued fraction [29] are applied to obtain the maximum convergence radius of the power series. In this study, the recursion form derived from the normalized Viskovatov method [29] is applied, which is presented in the Appendix-A in detail. Based on Stahl's approximation theory in [27] [28], the adoption of diagonal Padé approximants or continued fractions can (i) accelerate the speed of convergence and (ii) extend the convergence radius. Fig. 4 shows the block diagram of remote voltage control based on the HELM. Compared to Fig. 3, this approach does not update the impedances at each order, which avoids the calculation burden as needed in the N-R method for updating the Jacobian matrix at each iteration. Moreover, it does not require a separate dispatch step to dispatch reactive power contributions among different reactive power resources for the PVQ/P groups.

$$\begin{bmatrix}G_{pq,pq}&-B_{pq,pq}&-B_{pq,pv}&0&-B_{pq,pvq}&0&G_{pq,p}&-B_{pq,p}\\ B_{pq,pq}&G_{pq,pq}&G_{pq,pv}&0&G_{pq,pvq}&0&B_{pq,p}&G_{pq,p}\\ B_{pv,pq}&G_{pv,pq}&G_{pv,pv}&\mathbf{I_{pv,pv}}&G_{\boldsymbol{\mathcal{PV}},pvq}&0&B_{pv,p}&G_{pv,p}\\ G_{pv,pq}&-B_{pv,pq}&-B_{pv,pv}&0&-B_{pv,pvq}&0&G_{pv,p}&-B_{pv,p}\\ B_{pvq,pq}&G_{pvq,pq}&G_{pvq,pv}&0&G_{pvq,pvq}&0&B_{pvq,p}&G_{pvq,p}\\ G_{pvq,pq}&-B_{pvq,pq}&-B_{pvq,pv}&0&-B_{pvq,pvq}&0&G_{pvq,p}&-B_{pvq,p}\\ G_{p,pq}&-B_{p,pq}&-B_{p,pv}&0&-B_{p,pvq}&0&G_{p,p}&-B_{p,p}\\ B_{p,pq}&G_{p,pq}&G_{p,pv}&0&G_{p,pvq}&\mathbf{K_{p,pvq}}&B_{p,p}&G_{p,p}\end{bmatrix}\begin{bmatrix}V_{pq,re}[m]\\ V_{pq,im}[m]\\ V_{pv,im}[m]\\ \mathbf{Q_{pv}}[m]\\ V_{pvq,im}[m]\\ \mathbf{Q_p}[m]\\ V_{p,re}[m]\\ V_{p,im}[m]\end{bmatrix}$$
$$=\begin{bmatrix}\mathrm{Re}(\boldsymbol{\mathcal{PQ}}[m-1])\\ \mathrm{Im}(\boldsymbol{\mathcal{PQ}}[m-1])\\ \mathrm{Im}(\boldsymbol{\mathcal{PV}}[m-1])\\ \mathrm{Re}(\boldsymbol{\mathcal{PV}}[m-1])\\ \mathrm{Im}(\boldsymbol{\mathcal{PVQ}}[m-1])\\ \mathrm{Re}(\boldsymbol{\mathcal{PVQ}}[m-1])\\ \mathrm{Re}(\boldsymbol{\mathcal{P}}[m-1])\\ \mathrm{Im}(\boldsymbol{\mathcal{P}}[m-1])\end{bmatrix}-\begin{bmatrix}G_{pq,pv}\\ B_{pq,pv}\\ B_{pv,pv}\\ G_{pv,pv}\\ B_{pvq,pv}\\ G_{pvq,pv}\\ G_{p,pv}\\ B_{p,pv}\end{bmatrix}\cdot V_{pv,re}[m]-\begin{bmatrix}G_{pq,pvq}\\ B_{pq,pvq}\\ B_{pv,pvq}\\ G_{pv,pvq}\\ B_{pvq,pvq}\\ G_{pvq,pvq}\\ G_{p,pvq}\\ B_{p,pvq}\end{bmatrix}\cdot V_{pvq,re}[m] \tag{39}$$

$$\mathbf{K_{p,pvq}}=\begin{bmatrix}\mathbf{K}_1&&&&&\\ &\mathbf{K}_2&&&&\\ &&\ddots&&&\\ &&&\mathbf{K}_t&&\\ &&&&\ddots&\\ &&&&&\mathbf{K}_{N_{pvq}}\end{bmatrix}^{N_p\times N_{pvq}} \tag{40}$$

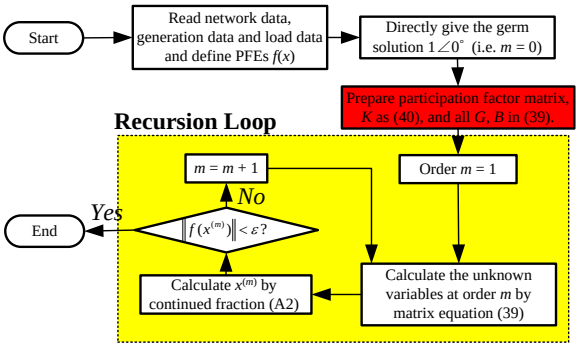

Fig. 4. Block diagram of joint remote voltage control based on the HELM.

IV. Case Study

The proposed HELM-based remote voltage control is tested on the IEEE New England 39-bus system, as shown in Fig. 5. The system is modified to have two remote voltage controllers (two PVQ/P groups). Gen 31 and Gen 32 remotely control the voltage magnitude at Bus 11 and Gen 35 and Gen 36 remotely control the voltage magnitude at Bus 22, marked as Blue and Green in Fig. 5. To demonstrate this approach in the case

U.S. Government work not protected by U.S. copyright.

This article has been accepted for publication in a future issue of this journal, but has not been fully edited. Content may change prior to final publication. Citation information: DOI 10.1109/TSG.2019.2901865, IEEE Transactions on Smart Grid

study, the values in the participation matrix are determined by the capacities of generators, i.e. $\kappa_{1,1}$= 0.468, $\kappa_{1,2}$= 0.532, $\kappa_{2,1}$= 0.537 and $\kappa_{1,2}$= 0.463. Nevertheless, for industrial applications, these values can be determined by optimizations on reactive power contributions to control the voltage at a common bus [30]. Other generators control the voltage magnitudes of their terminal buses. Bus 39 is the slack bus.

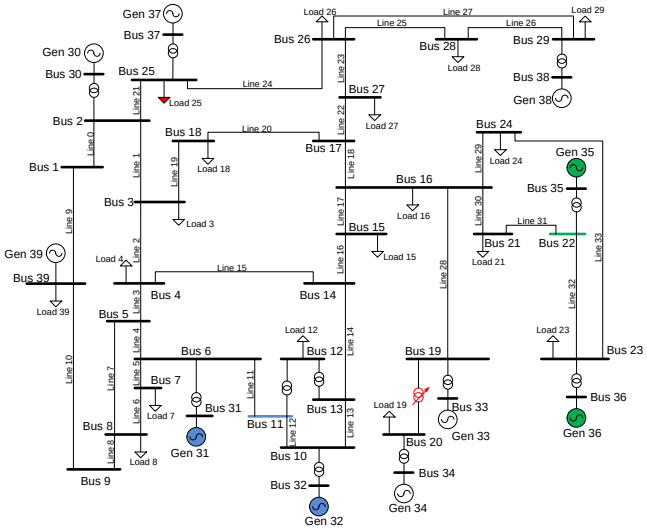

Fig. 5. IEEE New England 39-bus system modified for the case studies.

Case studies are carried out using the HELM programmed in the MATPOWER 4.1 [31] on a laptop with an Intel® Core i7-4600M dual 2.9 GHz processor and 16 GB RAM. For the sake of simplification, no reactive power limits of the generators are considered in the case studies. If reactive power limits are considered, the HELM-based remote voltage control needs to be rebuilt and resolved with altered bus types as the reactive power violates the limits at a certain P bus or PV bus. The procedure is the same with the N-R method in this aspect.

A. Simulations with the HELM

In the study case, the active power load at Bus 25 is increased from 224 MW until the power flow calculation fails to converge. Every incremental step is 100 MW. The HELM is adopted to find the power flow solution for every scenario with power mismatches of all buses less than a tolerance of 1×10^{-5}. If the largest power mismatch cannot meet the tolerance within 60 orders, then it is a non-convergence case.

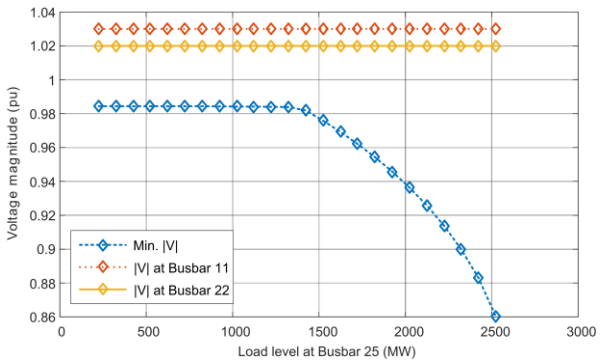

Fig. 6. The voltage magnitudes as the load increases at Bus 25.

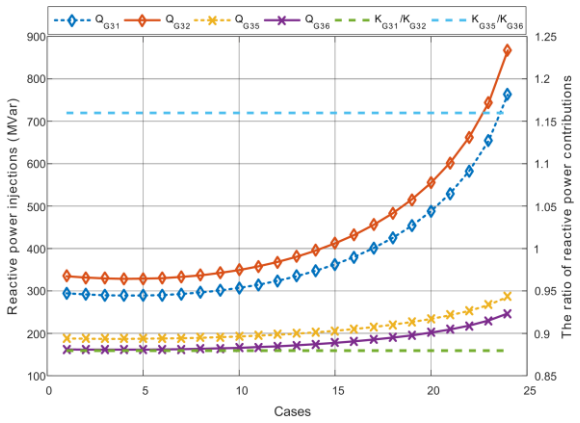

Fig. 7. The reactive power contribution at P buses.

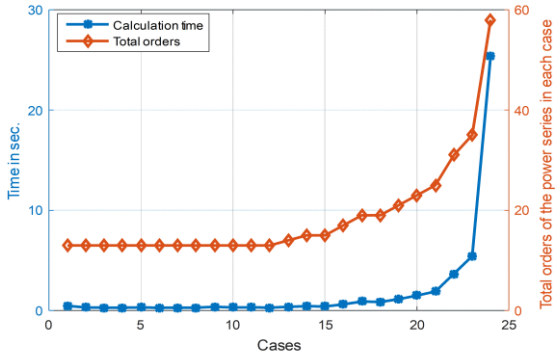

Fig. 8. The total required power series orders and the time consumption.

As shown in Fig. 6, the system voltage collapses when the load at Bus 25 increases beyond 2500 MW. In the HELM, the calculations start from the germ solution $1\angle0^{\circ}$ p.u. without an initial guess. For all different load levels at Bus 25, the voltage magnitudes at PVQ buses, i.e. Bus 11 and Bus 22, are kept constant due to the remote voltage control functions.

The reactive power outputs from P buses, Gen 31, Gen 32, Gen 35 and Gen 36 are shown in Fig. 7. Their reactive power contributions are predefined by participation factors, i.e. 1.16 for the ratio of Gen 31 to Gen 32 and 0.88 for the ratio of Gen 35 to Gen 36, respectively. The participation factors are kept constant for all scenarios. It demonstrates that the reactive power contributions from different P buses controlling the corresponding PVQ buses are controlled as expected.

Fig. 8 shows the total required orders of power series to converge to the power flow solution with the error tolerance 1×10^{-5}. It can be observed that more power series orders are needed when the system is approaching to the break point. The calculation time is also increased with the increase of load level. However, the convergence process can be much faster and much less power series orders are needed if transferring the power series into continued fractions by the normalized Viskovatov method [29].

B. Remote Voltage Control Using HELM vs. N-R Method

As discussed in previous sections, once the coefficients are found, either the summation of the power series at s = 1 or the

U.S. Government work not protected by U.S. copyright.

This article has been accepted for publication in a future issue of this journal, but has not been fully edited. Content may change prior to final publication. Citation information: DOI 10.1109/TSG.2019.2901865, IEEE Transactions on Smart Grid

continued fractions can be applied to obtain the values of system states, e.g. V_i and Q_i.

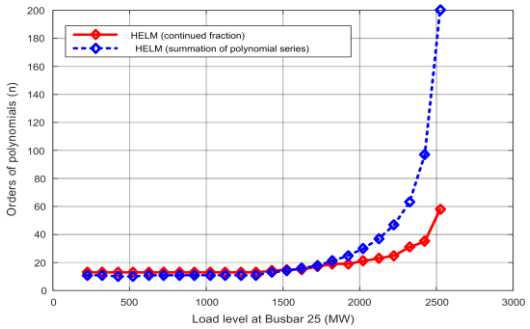

Fig. 9. The required orders of summation of the power series vs. the continued fractions with the same error tolerance, i.e. 1×10^{-5}.

Fig. 9 compares the required orders of power series and that of the continued fractions for a converged solution for various scenarios. As the active power consumption at Bus 25 increasing towards 2500 MW, the system is approaching to the critical point. More and more power series orders are needed to obtain the converged solutions. For the low load scenarios, i.e. the active power consumption at Bus 25 lower than 1700 MW, the summation of power series is more efficient to obtain the solutions. In contrast, for the high load scenarios, the continued fraction is more preferable to obtain the solutions with fewer orders than the direct summation.

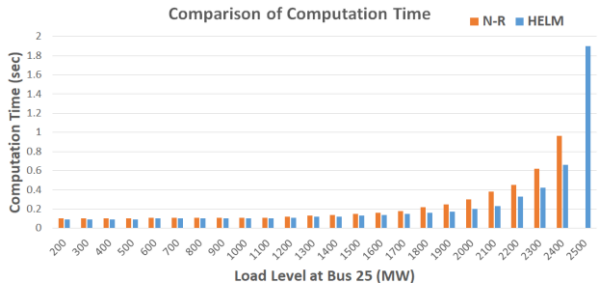

Fig. 10. Comparison of computation time of the N-R method and HELM with the same error tolerance, i.e. 1×10^{-8}.

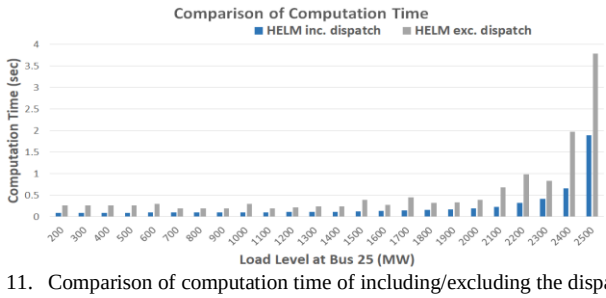

Fig. 11. Comparison of computation time of including/excluding the dispatch step in/from the HELM formulation with the same error tolerance, i.e. 1×10^{-8}.

Fig. 10 compares the computation time of the N-R method and HELM for different load levels at Bus 25. Both methods are implemented in MATLAB and tested on a desktop computer with Intel Core i7-6700 CPU (4 cores) at 3.40 GHz and 16 GB RAM. Continued fractions using Viskovatov method are applied to obtain the maximum convergence radius. The calculation of continued fraction uses the parallel computing toolbox that fully utilizes the 4 cores. For the low load scenarios, the computation time of HELM is slightly shorter than the N-R method. For the higher load scenarios, the HELM is much faster than the N-R method. When the active power consumption at Bus 25 approaches 2500 MW, the N-R method is unable to converge while the HELM converges in 1.897sec.

Fig. 11 compares the computation times for different load levels at Bus 25, using the proposed method and the conventional HELM excluding the dispatching step for remote voltage control. Note that the proposed method directly includes the dispatching step in the HELM formulation, i.e. Eq. (39), while the previous method excludes the dispatching step as an outer loop, similar to the N-R method. Thus, the HELM is solved several times, and reactive power is dispatched and updated each time. It can be noticed that the computation speed is 2-3 times higher, if including the dispatching step in the HELM formulation.

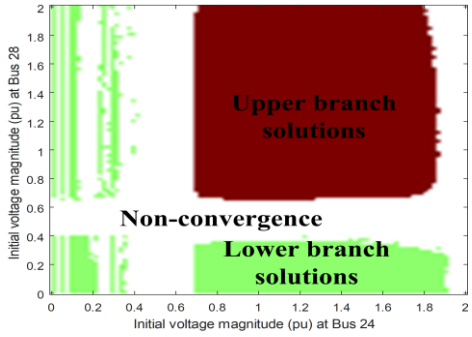

Fig. 12. Case A: convergence map on different initial points for total 101×101 power flow calculations by the N-R method (Red: upper-branch solutions; Green: lower-branch solutions; White: non-convergence region).

As introduced in Section III, the HELM is superior to iterative methods in its independence of the initial guess. Also, it guarantees the convergence to a set of stable, upper-branch power flow solutions from a given germ solution $1\angle0^\circ$ p.u. Case A is the basic operating condition. Fig. 12 shows the map of convergence by N-R method with respect to different initial guesses. Each pixel in the map represents a power flow calculation with different initial voltage magnitudes at Bus 24 and Bus 28, which vary from 0 to 2 p.u. at 0.02 p.u. intervals, so a total number of 101×101 power flow calculations are carried out. Although the initialization with a voltage range of 0.8-1.2pu can ensure convergent solutions in this study, it cannot ensure the convergence of the initialization from this range for large-scale power systems with lots of control functions. Initial points from the red region can converge to the stable solutions on the upper-branch of P-V curves, while that from the green region converges to the unstable solutions on the low-branch of P-V curves. White region is the non-convergence region. In contrast, the HELM does not depend on any "initial guess". The germ solution for voltage at $1\angle0^\circ$ p.u. always serves as the initial point and the final solution is guaranteed to be an "upper branch solution". Note that a solution is stable only if the eigenvalues of its Jacobian matrix. All have negative real parts [32]. The solutions obtained by HELM are confirmed to be stable and always on upper branches of P-V curves at all buses.

U.S. Government work not protected by U.S. copyright.

This article has been accepted for publication in a future issue of this journal, but has not been fully edited. Content may change prior to final publication. Citation information: DOI 10.1109/TSG.2019.2901865, IEEE Transactions on Smart Grid

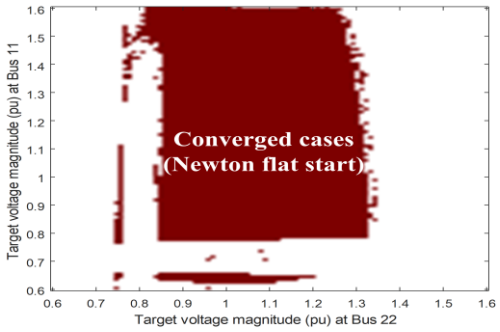

Fig. 13. Case B: the convergence map of the N-R method in the test grid with different voltage magnitudes at two PVQ buses.

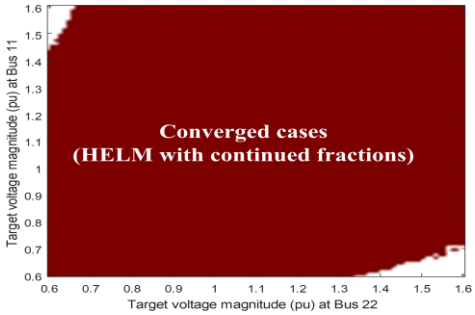

Fig. 14. Convergence map of HELM about voltage magnitudes of two PVQ buses, whose target voltage magnitudes vary 0.6-1.6pu with 0.01pu intervals.

In Case B, the system's operating condition is changed, i.e. the active power and the reactive power consumptions at Bus 25 is changed to 100 MW and 500 MVar, respectively. The target voltage magnitudes at PVQ buses, i.e. Bus 11 and Bus 22, vary from 0.6 p.u. to 1.6 p.u. with 0.01 p.u. intervals. A total number of 101×101 power flow calculations are also carried out. Fig. 13 and Fig. 14 show the convergence maps of the N-R method with the flat start and the HELM with the continued fraction, respectively. Both the maximum iteration number of the N-R method and the maximum order of the HELM's power series are set to 50. It is apparent that the convergence region by the HELM in Fig. 14 is much larger than that by the N-R method in Fig. 13. Moreover, the solutions based on the HELM can be guaranteed to be the stable power flow solution, but the solutions based on N-R method may be the unstable equilibrium points.

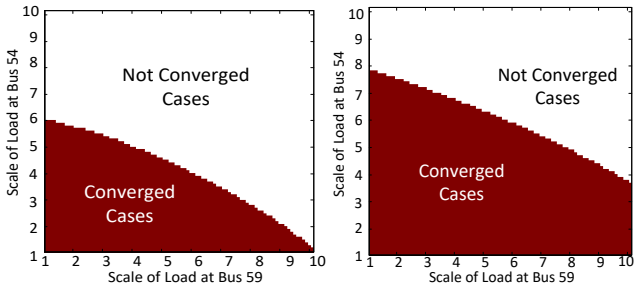

(a) N-R method (b) HELM

Fig. 15. Convergence maps of two methods about loading scales at Bus 54 and Bus 59 with intervals 0.1 and the error tolerance i.e. 1×10^{-8}.

In Case C, the proposed HELM-based remote voltage control is also tested on the IEEE 118-bus system. The system is also modified to have two remote voltage controllers (two PVQ/P groups). Gen 65 and Gen 66 remotely control the voltage magnitude at Bus 67 and Gen 36 and Gen 40 remotely control the voltage magnitude at Bus 37. The convergence maps for the loading scales of Bus 54 and Bus 56 are shown in Fig. 15 for the traditional N-R method and proposed HELM. Both methods are set with the error tolerance 1×10^{-8} p.u.. It can be observed that the HELM performs significantly better when the operating conditions are close to the instability boundary in terms of convergence.

V. Conclusion

This paper proposes a remote voltage control function using the non-iterative HELM to online control the voltage magnitude of remote buses. A general voltage control function is introduced in the HELM, in which the voltage magnitudes at specific buses are controlled by multiple reactive power resources from remote buses. A participation factor matrix is integrated into the HELM to distribute the reactive power contribution among multiple reactive power resources.

The simulations implemented in the IEEE New England 39-bus system demonstrate that the HELM integrated with the participation factor matrix has better performance in convergence than the traditional N-R method embedded with the remote voltage control function.

The key findings of this paper include: 1) the proposed HELM has a non-iterative feature and a larger convergence region to guarantee finding a correct operational solution, and hence is more suitable for remote voltage control. 2) The computation speed of the proposed HELM is faster than a traditional method thanks to its capability of distributing the computations of continued fractions among multiple parallel processors. The future research on this approach includes 1) using passive elements, i.e. tap-changers, shunts for remote voltage control; 2) deriving the optimal trajectory of remote voltage control; 3) exploring the N-R method for remote voltage control with integrated dispatching steps.

Appendix

A. Viskovatov Method to From Continued Fraction

The voltage at each bus is modelled as a power series w.r.t embedded variable s, i.e.

$$V = C[0] + C[1]s + C[2]s^2 + \cdots + C[m]s^m \tag{A1}$$

where $C[m]$ are the coefficients of the power series.

The power series (A1) can be converted to the continued fraction in (A2) by Viskovatov method [29]. In the proposed HELM, the voltages at $s = 0$ are $1\angle0^\circ$, therefore $C[0] = 1$.

$$V = C[0] + \underset{m=1}{\overset{\infty}{\mathbf{K}}}\left(\frac{\overline{C}_{m0}}{1}\right) = C[0] + \cfrac{\overline{C}_{10}}{1+\cfrac{\overline{C}_{20}}{1+\cfrac{\overline{C}_{30}}{1+\cdots}}}, \tag{A2}$$

$$\text{and } \overline{C}_{m0} \neq 0, \ \forall m \geq 1$$

where $\mathbf{K}$ represents the continued fraction operator. $\overline{C}_{m0}$ are the numerator of the m^{th} degree of the continued fraction. For each bus, the variables can be obtained at $s = 1$. The coefficient of continued fractions can be solved by a matrix

U.S. Government work not protected by U.S. copyright.

This article has been accepted for publication in a future issue of this journal, but has not been fully edited. Content may change prior to final publication. Citation information: DOI 10.1109/TSG.2019.2901865, IEEE Transactions on Smart Grid

(A3). The first and the second rows are filled with the power series coefficients. The other elements of (A3) can be derived by (A4) [29].

$$\begin{bmatrix} 1 & 0 & 0 & 0 & 0 & \cdots \\ C[1] & C[2] & C[3] & C[4] & C[5] & \cdots \\ \overline{C}_{2,0} & \overline{C}_{2,1} & \overline{C}_{2,2} & \overline{C}_{2,3} & \overline{C}_{2,4} & \cdots \\ \overline{C}_{3,0} & \overline{C}_{3,1} & \overline{C}_{3,2} & \overline{C}_{3,3} & \overline{C}_{3,4} & \cdots \\ \overline{C}_{4,0} & \overline{C}_{4,1} & \overline{C}_{4,2} & \overline{C}_{4,3} & \overline{C}_{4,4} & \cdots \\ \vdots & \vdots & \vdots & \vdots & \vdots & \ddots \end{bmatrix} \tag{A3}$$

$$\overline{C}_{m,j} = \overline{C}_{m-2,j+1} \Big/ \overline{C}_{m-2,0} - \overline{C}_{m-1,j+1} \Big/ \overline{C}_{m-1,0}, \quad \forall m \geq 2 \text{ and } j \geq 0 \tag{A4}$$

The recursive form of continued fractions is then applied:

$$\begin{bmatrix} A_m \\ B_m \end{bmatrix} := \begin{bmatrix} A_{m-1} \\ B_{m-1} \end{bmatrix} + \overline{C}_{m,0} \begin{bmatrix} A_{m-2} \\ B_{m-2} \end{bmatrix}, \quad \text{and} \quad \overline{C}_{m0} \neq 0, \ \forall m \geq 1 \tag{A5}$$

where A_{-1}: = 1, B_{-1}: = 0, A_0: = C[0] and B_0: = 1. Finally, the voltage at each bus is calculated by

$$V = A_m \Big/ B_m \tag{A6}$$

where m is the maximum order of continued fractions.

B. Proof of Convergence to the Upper-Branch Solution

For an N-bus network with different bus types, the voltage of each bus (excluding the slack bus) can be extended to the following form [33], in particular with C[0] = 1 in (A2).

$$V_i(s) = 1 + \frac{s\sigma_i(s)}{V_i^*(s^*)} = 1 + \cfrac{s\sigma_i(s)}{1 + \cfrac{s\sigma_i^*(s^*)}{1 + \cfrac{s\sigma_i(s)}{1+\cdots}}} \tag{A7}$$

where $\sigma_i(s)$ is the complex equivalent parameter to be determined for bus i. Therefore, if the procedure of HELM with remote voltage control stops at the m^{th} orders of power series, as shown in (A1), the explicit form of voltage at bus i is (A6), whose coefficients are obtained by (A5), with

$$\overline{C}_{m,0} = \begin{cases} s\sigma_i(s) & m = 2k-1 \\ s\sigma_i^*(s^*) & m = 2k \end{cases} \quad k \in \mathbb{N} \tag{A8}$$

Then, the even and odd terms of numerator and denominator of (A5) are separated as (A9), so there is (A10)

$$\begin{aligned} A_{2m+1}(s) &= A_m^{(-)}(s); \quad B_{2m+1}(s) = B_m^{(-)}(s); \\ A_{2m}(s) &= A_m^{(+)}(s); \quad B_{2m+1}(s) = B_m^{(+)}(s); \end{aligned} \tag{A9}$$

$$\begin{aligned} A_{m+1}^{(+)}(s) - \left(1 + 2s\sigma_R(s)\right) A_m^{(+)}(s) + s^2 \left(\sigma_R(s)^2 + \sigma_I(s)^2\right) A_{m-1}^{(+)}(s) = 0 \\ B_{m+1}^{(+)}(s) - \left(1 + 2s\sigma_R(s)\right) B_m^{(+)}(s) + s^2 \left(\sigma_R(s)^2 + \sigma_I(s)^2\right) B_{m-1}^{(+)}(s) = 0 \end{aligned} \tag{A10}$$

where $\sigma_R(s)$ and $\sigma_I(s)$ are respectively the real and imaginary parts of $\sigma_i(s)$. The limit of quotient of numerator terms is defined by a new variable γ,

$$\lim_{m\to\infty} \left. \frac{A_m^{(+)}(s)}{A_{m-1}^{(+)}(s)} \right|_s \equiv \gamma \tag{A11}$$

which can be solved by finding the roots of quadratic characteristic polynomial.

$$\gamma^2 - \left(1 + 2s\sigma_R(s)\right)\gamma + s^2 \left(\sigma_R(s)^2 + \sigma_I(s)^2\right) = 0 \tag{A12}$$

$$\gamma_\pm = \frac{1}{2} + s\sigma_R(s) \pm \sqrt{\frac{1}{4} + s\sigma_R(s) - s^2\sigma_I(s)^2} = \frac{1}{2} + s\sigma_R(s) \pm \Delta(s) \tag{A13}$$

Therefore, if the germ solution has all voltages at $1\angle 0^\circ$ p.u., then A_0 = 1 and B_0 = 1. One can compute the limit when $n \to \infty$ of the continued fraction as

$$\lim_{m\to\infty} V_m^+(s) = \lim_{m\to\infty} V_{2m}(s) = \frac{A_m^{(+)}(s)}{B_m^{(+)}(s)} = \frac{\gamma_+}{\gamma_+ - s\sigma(s)} = \frac{\frac{1}{2} + s\sigma_R(s) + \Delta(s)}{\frac{1}{2} + s\sigma_R(s) + \Delta(s) - s\sigma(s)} \tag{A14}$$

which can be derived to

$$\lim_{m\to\infty} V_m^+(s) = \frac{1}{2} + \Delta(s) + js\sigma_I(s) = \frac{1}{2} + \sqrt{\frac{1}{4} + s\sigma_R(s) - s^2\sigma_I(s)^2} + js\sigma_I(s) \tag{A15}$$

(A15) only has the positive solution, which is exactly the final result of the upper-branch solution of PV curves. ■

VI. REFERENCES

[1] *Technical Regulation 3.2.5 for Wind Power Plants above 11kW*, Energinet.dk. Jan. 2017.

[2] N. Qin, C. L. Bak, et al, "Multi-stage optimization-based automatic voltage control systems considering wind power forecasting errors," *IEEE Trans. Power Syst.*, vol. 32, no. 2, pp. 1073-1088, Mar. 2017.

[3] M. D. Ilic, et al, "Improved secondary and new tertiary voltage control," *IEEE Trans. Power Systems*, vol. 10, no. 4, pp. 1851-1862, Nov. 1995.

[4] W. Tinney, C. E. Hart, "Power flow solution by Newton's method," *IEEE Trans. Power Apparatus and Systems*, vol. PAS-86, no.11, pp. 1449-1460, Nov. 1967.

[5] S. C. Tripathy *et al.*, "Load-flow solutions for ill-conditioned power systems by a Newton-like method," *IEEE Transactions on Power Apparatus and Systems*, vol. PAS-101, no.10, pp. 3648-3657, Oct. 1982.

[6] A. Trias, "The holomorphic embedding load flow method," *IEEE PES GM*, San Diego, CA, Jul. 2012.

[7] A. Trias, "System and method for monitoring and managing electrical power transmission and distribution networks," US Patents 7 519 506 and 7 979 239, 2009-2011.

[8] A. Trias, "Fundamentals of the holomorphic embedding load–flow method" *arXiv: 1509.02421v1*, Sep. 2015.

[9] M. K. Subramanian, "Application of holomorphic embedding to the power-flow problem," *Master Thesis*, Arizona State Univ., Aug. 2014.

[10] S. S. Baghsorkhi, S. P. Suetin, "Embedding AC power flow with voltage control in the complex plane: the case of analytic continuation via Padé approximants," *arXiv:1504.03249*, Mar. 2015.

[11] M. K. Subramanian *et al.*, "PV bus modeling in a holomorphically embedded power-flow formulation," *North American Power Symposium (NAPS)*, Manhattan, KS, 2013.

[12] I. Wallace *et al.*, "Alternative PV bus modelling with the holomorphic embedding load flow method," *arXiv:1607.00163*, Jul. 2016

[13] S. S. Baghsorkhi *et al.*, "Embedding AC power flow in the complex plane part I: modelling and mathematical foundation," *arXiv:1604.03425*, Jul. 2016

[14] S. Rao *et al.*, "The holomorphic embedding method applied to the power-flow problem," *IEEE Trans. Power Syst.*, vol. 31, no. 5, pp. 3816-3828, Sep. 2016.

[15] C. Liu, B. Wang, X. Xu, K. Sun, D. Shi, C. L. Bak, "A multi-dimensional holomorphic embedding method to solve AC power flows," *IEEE Access*, vol. 5, pp. 25270-25285, Nov. 2017.

[16] C. Liu, B. Wang, F. Hu, K. Sun, C. L. Bak, "Online voltage stability assessment for load areas based on the holomorphic embedding method," *IEEE Trans. Power Syst.*, in press.

[17] B. Wang, C. Liu, K. Sun, "Multi-stage holomorphic embedding method for calculating the power-voltage curve," *IEEE Trans. Power Syst.*, vol. 33, no. 1, pp. 1127-1129, Jan. 2018.

[18] C. Liu, K. Sun, B. Wang, W. Ju, "Probabilistic power flow analysis using the multi-dimensional holomorphic embedding and generalized cumulants," *IEEE Trans. Power Syst.*, vol. 33, no. 6, pp. 7132-7142, Nov. 2018.

[19] A. Trias, J. L. Marin, "The holomorphic embedding loadflow method for DC power systems and nonlinear DC circuits," *IEEE Trans. Circuits and Systems-I: regular papers*, vol. 63, no.2, pp. 322-333, Sep. 2016.

U.S. Government work not protected by U.S. copyright.

This article has been accepted for publication in a future issue of this journal, but has not been fully edited. Content may change prior to final publication. Citation information: DOI 10.1109/TSG.2019.2901865, IEEE Transactions on Smart Grid

[20] Y. Feng and D. Tylavsky, "A novel method to converge to the unstable equilibrium point for a two-bus system," *North American Power Symposium (NAPS)*, Manhattan, KS, 2013.
[21] S. Rao, D. Tylavsky, "Nonlinear network reduction for distribution networks using the holomorphic embedding method," *North American Power Symposium (NAPS)*, Denver, CO, USA, 2016.
[22] D. S. Popovic, V. A. Levi, "Extension of the load flow model with remote voltage control by generator," *Electric Power Systems Research*, vol. 25, no. 3, pp. 207-212, Dec. 1992.
[23] Y. Guo *et al.*, "Solvability and solutions for bus-type extended load flow," *Electric Power & Energy Systems*, vol. 51, pp. 89-97, Dec. 2013.
[24] A. Conejo *et al.*, "A nonlinear approach to the selection of pilot buses for secondary voltage control," in Proc. of *the 4th Int. Conf. on Power System Control and Management*, pp. 191-195, London, Apr. 1996.
[25] S. Colombo, *Holomorphic Functions of One Variable*, Gordon and Breach Science Publishers Inc., New York, 1983.
[26] M. R. Range, *Holomorphic Functions and Integral Representations in Several Complex Variables*, Springer-Verlag, New York, Inc. 2002.
[27] H. Stahl, "On the convergence of generalized Padé approximants," Constructive Approximation, vol. 5, pp. 221-240, 1989.
[28] H. Stahl, "The convergence of Padé approximants to functions with branch points," *Journal of Approximation Theory*, vol. 91, no. 2, pp. 139-204, 1997.
[29] A. Cuyt *et al.*, "Handbook of Continued Fractions for Special Functions," *Springer*, ISBN: 978-1-4020-6948-2.
[30] J. L. Sancha *et al.*, "Spanish practices in reactive power management and voltage control," Proc. of *IEE Colloquium on International Practices in Reactive Power Control*, London, UK, Apr. 1993.
[31] R. D. Zimmerman *et al.*, "MATPOWER: Steady-State Operations, Planning and Analysis Tools for Power Systems Research and Education," *IEEE Trans. Power Syst.*, vol. 26, no. 1, pp. 12-19, Feb. 2011.
[32] H. D. Chiang, F. F. Wu, P. P. Varaiya, "Foundations of direct methods for power system transient stability analysis," *IEEE Trans. Power on Circuits and Systems.*, vol. CAS-34, no. 2, pp. 160-173, Feb. 1987.
[33] S. Rao *et al.*, "Estimating the saddle-node bifurcation point of static power series using the holomorphic embedding method," *Electric Power and Energy Systems.*, vol. 84, pp. 1-12, Jan. 2017.

Chengxi Liu (S'10_M'13_SM'18) received the B.Eng. and M.Sc. degrees from the Huazhong University of Science and Technology, Wuhan, China, in 2005 and 2007, respectively, and the Ph.D. degree from the Department of Energy Technology, Aalborg University, Aalborg, Denmark, in 2013. He was with Energinet.dk, the Danish TSO until 2016. He was a Research Associate with the Department of Electrical Engineering and Computer Science, The University of Tennessee, USA, from 2016 to 2018. He is currently an Associate Professor with the Department of Energy Technology, Aalborg University. His research interests include stability and control of power systems, simulation methods of power systems, and big data and artificial intelligence applied in power systems.

Nan Qin was born in Beijing, China, 1983. He received his B.Eng. degree in automation technology from Beijing University of Technology, Beijing, China, in 2006, the B.Eng. degree in I.T. from Mikkeli University of Applied Sciences, Mikkeli, Finland, in 2009, the M.Sc. degree in E.E. from the Technical University of Denmark, Lyngby, Denmark, in 2009 and Ph.D. in energy technology from Aalborg University, Aalborg, Denmark in 2016. He is currently working in the Danish Transmission System Operator, Energinet, where he mainly works on system stability assessments for the grid planning and the operations, and participates in the COBRAcable HVDC project, Danish Automatic Voltage Control studies and the international consultancy projects on behalf of Energinet Energy Consultancy A/S.

Kai Sun (M'06–SM'13) received the B.S. degree in automation in 1999 and the Ph.D. degree in control science and engineering in 2004 both from Tsinghua University, Beijing, China. He is an associate professor at the Department of EECS, University of Tennessee, Knoxville, USA. He was a project manager in grid operations and planning at the EPRI, Palo Alto, CA from 2007 to 2012. Dr. Sun serves in the editorial boards of IEEE Transactions on Power Systems, IEEE Transactions on Smart Grid, IEEE Access and IET Generation, Transmission and Distribution.

Claus Leth Bak (M'99, SM'07) was born in Århus, Denmark, on April 13th, 1965. He received the B.Sc. with honors in Electrical Power Engineering in 1992 and the M.Sc. in Electrical Power Engineering at the Department of Energy Technology at Aalborg University in 1994. After his studies he worked as a professional engineer with Electric Power Transmission and Substations with specializations within the area of Power System Protection at the NV Net Transmission System Operator. In 1999 he was employed as an Assistant Professor at the Department of Energy Technology, Aalborg University, where he holds a Full Professor position today. He received the PhD degree in 2015. His main Research areas include Corona Phenomena on Overhead Lines, Composite Transmission Towers, Power System Modeling and Transient Simulations, Underground Cable transmission, Power System Harmonics, Power System Protection and HVDC-VSC Offshore Transmission Networks. He has over 300 publications. He is a member of Cigré SC C4 AG1 and SC B5 and was the chairman of the Danish Cigré National Committee. He received the DPSP 2014 best paper award and the PEDG 2016 best paper award.

U.S. Government work not protected by U.S. copyright.